The results of joint GBM-LAT spectral analysis of four fluence populations of GRBs

Saeeda Sajjad[1,2], Syed Ali Mohsin Bukhari[1,2], Iqra Siddique[1,2], Alina Nawaz[1,2], Hira Zafar[1,2]

[1]Department of Space Science, Institute of Space Technology, 44000 Islamabad, Pakistan,
[2]Space and Astrophysics Research Lab, National Centre of GIS and Space Applications, 44000 Islamabad, Pakistan

Abstract

The second Fermi LAT GRB catalog presents the results for 186 Gamma Ray Bursts (GRBs) detected by the Fermi Large Area Telescope (LAT) between 2008 and 2018. Out of these, we select the GRBs with significant detection in the LAT and GBM during the T90 time interval. We further subdivide this population into four quartiles based on the fluence from the GBM and carry out joint GBM-LAT spectral analysis for the T90 duration with single and multi-component spectral models. Here, we present the results for best fit model, spectral indices, Epeak and fluence obtained from the joint analysis. We also compare the spectral properties of the four quartiles

Introduction

The Fermi GBM and LAT provide a combined energy range coverage of 7 orders of magnitude from ~8 keV to ~300 GeV. This unprecedented coverage has allowed the identification of additional components such as an additional power law (PL) at high energies or a black body (BB) component in the spectra of many GRBs. However, several of the GRBs presented in the LAT second catalog (2FLGC) [1] have not been previously analysed jointly. Here, we present the results of the time integrated joint analysis of these GRBs.

Selected population

We analysed GRBs in the GBM T90 interval (T90 hereafter). The 2nd LAT catalog has 81 GRBs which triggered the GBM and also have significant detection in the LAT in this time window. We classified these GRBs in four quartiles based on the their fluence in the GBM in the T90 interval.

Fluence population	Total GRBs	Short	Long	Fluence range (erg/cm^2)
Low	22	8	16	10^{-7} - 10^{-5}
Medium low	19	1	18	10^{-5} - 3x10^{-5}
Medium high	20		20	3x10^{-5} - 8x10^{-5}
High	20		20	8x10^{-5} - 3x10^{-5}

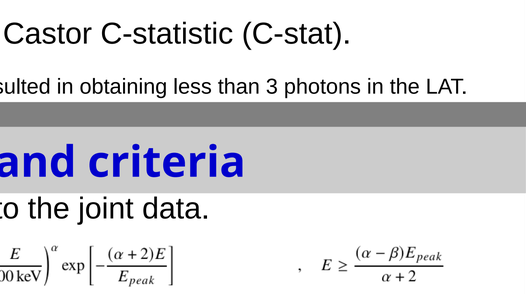

Method

GBM: 2 to 3 NaI + 1 or 2 BGO (for GRBs close to the GBM median) detectors with the smallest angle with the source were chosen. The refined GRB positions obtained in the LAT 2nd catalog were used. New response files (rsp2) were generated using GBMRSP v2.0 tool and GBM DRM database v2.0 database.
Energy selection: 8 to 900 keV (excluding 30-40 keV for iodine K-edge) for NaI and 250 keV to 40 MeV for BGO detectors.
Binning: TTE files with 0.064 s bins for GRBs with T90 < 300 s. CSPEC files with 1.024 s binning for GRBs with T90 > 300 s.

LAT unbinned likelihood analysis: The P8R3_TRANSIENT020E event class, and iso_P8R3_TRANSIENT020E_V2 and gll_iem_v07 for isotropic and galactic templates were used*. The 4th Fermi LAT source catalog was used to model the sources in a region of interest of 12° and source region of 30°. Earth limb contamination cut was set at 100°. For GRBs at zenith angles of 95°, a smaller ROI Of 8° and boresight angle cut of 105° were chosen.
Joint analysis: rmfit v4.3.2, with Castor C-statistic (C-stat).

***Note:** For 2 GRBs, these different choices resulted in obtaining less than 3 photons in the LAT.

Models and criteria

The following models were fitted to the joint data.

- Band
- Band + PL
- Band + BB
- Band+PL+BB

$$f_{Band}(E) = A \begin{cases} \left(\frac{E}{100\,\mathrm{keV}}\right)^{\alpha} \exp\left[-\frac{(\alpha+2)E}{E_{peak}}\right] & , \quad E \geq \frac{(\alpha-\beta)E_{peak}}{\alpha+2} \\ \left(\frac{E}{100\,\mathrm{keV}}\right)^{\beta} \left[\frac{(\alpha-\beta)E_{peak}}{100\,\mathrm{keV}(\alpha+2)}\right]^{\alpha-\beta} \exp(\beta-\alpha) & , \quad E < \frac{(\alpha-\beta)E_{peak}}{\alpha+2} \end{cases}$$

$$f_{PL}(E) = A\left(\frac{E}{E_{piv}}\right)^{\alpha} \qquad f_{BB}(E) = A\frac{E^2}{\exp\left(\frac{E}{kT}\right)-1}$$

Criteria

First, the presence of a PL component was determined by requiring that the addition of a PL improve the C-stat by 25. Then the resultant model was tested for the presence of an additional BB component by requiring a C-stat improvement of 25 as well.

Effective area correction

An Effective Area Correction factor (EAC) was also applied to account for the differences in calibration between the NaI and BGO detectors. If the addition of EAC improved the C-stat for the Band model by 9, then the EAC factor was kept in the steps described above

Constrained model criteria

The fits are also classified as constrained or not through the criteria established by Kaneko et al. [4] and used by Gruber et al. [3]. The relative error is required to be less than 1 for beta and less than 0.4 for all other parameters in the Band function. The criteria is not applied to the parameters of the additional components. The results with and without the application of this criteria are reported in the table.

Results

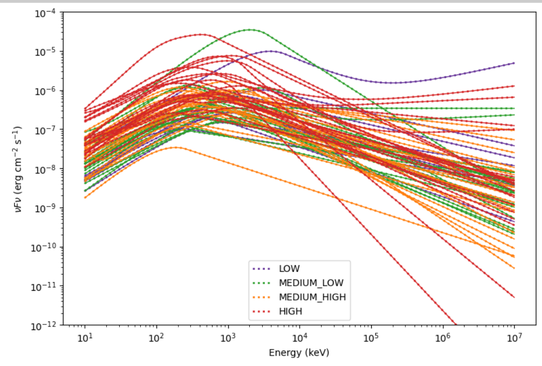

Fluence population	Total	Band fit[12]	Additional PL[12]	Additional BB[12]	Additional PL+BB[12]
Low	22	19 (8)	2 (1)		
Medium low	19	19 (18)	2 (1)	1 (0)	
Medium high	20	20 (20)	3 (1)	3 (2)	1 (0)
High	20	20 (20)	4 (4)	13 (10)	3 (3)
Total	**81**	**79 (66)**	**11 (7)**	**17 (12)**	**4 (3)**

[1]Converged fits, [2]Converged fits which also obey the constrained criteria

Parameters

The population wise distributions of fitted parameters (alpha, beta, Epeak) for all best fit models are shown. The sum of the distributions of all populations is shown in grey.

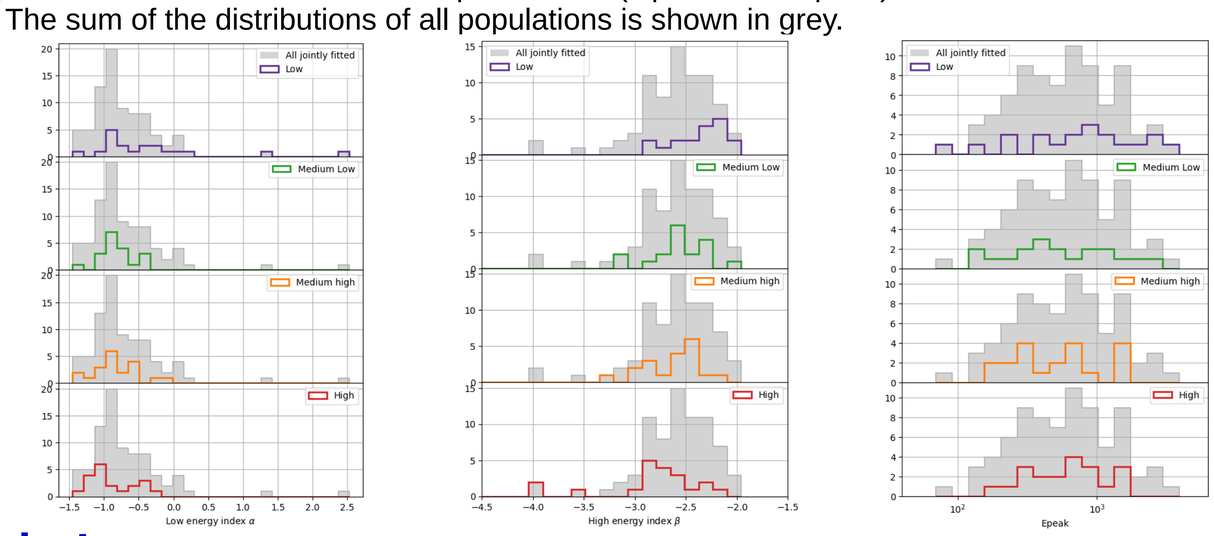

Correlations

The correlations for all best fit model parameters are shown in colour (constrained models only). For reference the distributions of parameters from the GBM catalog are also shown in grey.

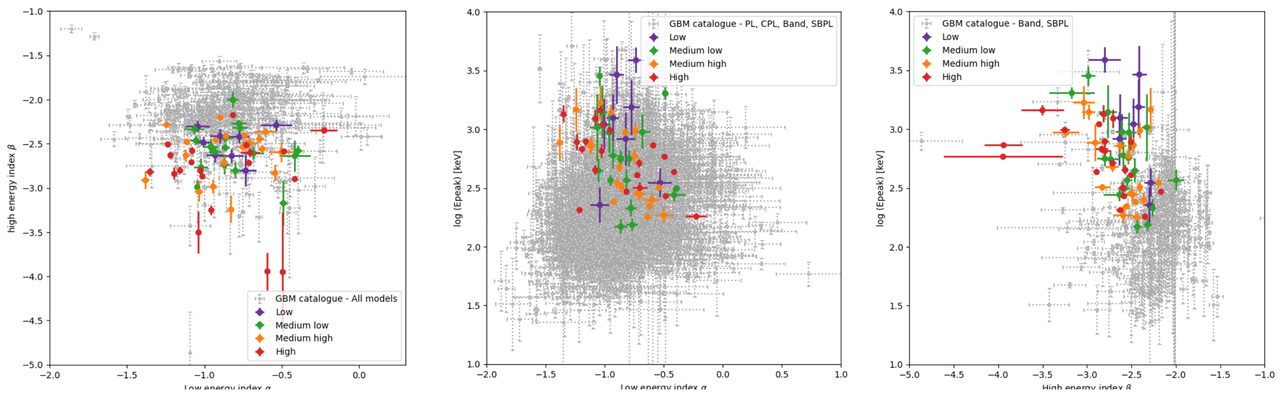

Fluence

The fluence obtained from the current study in the 10 keV- 10 GeV energy range (abcissae axis), is compared with the fluence in the GBM in T90 (left), LAT in T90 (centre) and LAT in the LAT time window (right). The last three values are obtained from the GBM [2] and LAT [1] catalogues respectively.

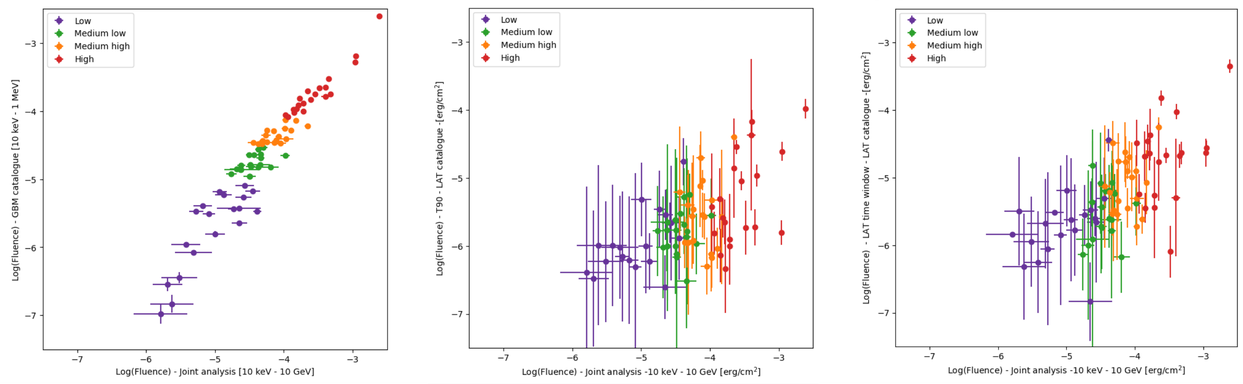

Summary and future directions

Eighty one GRBs were jointly analysed through their GBM and LAT data. The results show the presence of additional PL and BB components in at least 7 and 12 GRBs of the lot. In the low fluence category range, the fits are harder to constrain and the parameters show more deviations from typical values. Comparisons with the fits from the GBM only data seem to indicate that the jointly fitted GRBs tend to have larger Epeak and steeper beta values. These trends need to be verified through further comparisons and fits carried out with more base models such as Cut-off Power Law (CPL) and Smoothly Broken Power Law (SBPL). Lower fluence population GRBs show a greater change in fluence through the addition of the LAT data

Acknowledgements

The authors would like to thank Soebur Razzaque, Judy Racusin, Frédéric Piron and Feraol Fana Dirirsa for their valuable advice and discussions.

References

[1] Ajello, M., et al. "A decade of gamma-ray bursts observed by Fermi-LAT: the second GRB catalog." The Astrophysical Journal 878.1 (2019): 52.
[2] Bhat, P. Narayana, et al. "The third fermi GBM gamma-ray burst catalog: the first six years." The Astrophysical Journal Supplement Series 223.2 (2016): 28.
[3] Gruber, David, et al. "The Fermi GBM gamma-ray burst spectral catalog: four years of data." The Astrophysical Journal Supplement Series 211.1 (2014): 12.
[4] Kaneko, Yuki, et al. "The complete spectral catalog of bright BATSE gamma-ray bursts." The Astrophysical Journal Supplement Series 166.1 (2006): 298.